2022 학년도 전기[2023 년 2 월]

이학사학위 논문

Relationship Between Nearby Galaxy Clusters Mass ($0.01 < z < 0.2$) And Their Brightest Cluster Galaxies (BCGs)

논문지도교수 : 이명균 (인)

논문심사교수 : 손주비 (인)

이 논문을 이학학사 학위논문으로 제출함.

2023 년 2 월

서울대학교 자연과학대학 물리·천문학부 천문학전공

２０１４－１９４０２ 박 철 준

Abstract

The goal of this paper is to propose an easy way to estimate the galaxy clusters' mass with their brightest cluster galaxies (BCGs), which is recently considered an important part of galaxy research. So, I investigate connections between BCGs and their clusters. First of all, I choose a GalWCat19 cluster sample including 1,800 clusters within 0.02 < z < 0.2 and 34,471 cluster membership galaxies from SDSS dr13. It is significant to find the relation among physical properties and photometric data (magnitude) of an elliptical galaxy, which is the type of BCG, to fill missing physical values offered by the SDSS spectroscopic research database tables. With complete SDSS dataset and GalWCat19 data, I examine the cluster dynamical mass (M_{200}; within Δ(overdensity)=200) relations to BCG's stellar mass ($M_{*,BCG}$), velocity dispersion ($\sigma_{*,BCG}$) and absolute magnitude ($M_{K,BCG}$; instead of luminosity). The observed relation between $M_{*,BCG}$ and M_{200} is tight. The result is given as: $\log(M_{*,BCG}) = (0.21 \pm 0.03)\ \log M_{200} + (8.55 \pm 0.37)$. In addition, the relations between ($\sigma_{*,BCG}$, $M_{K,BCG}$) and M_{200} is also slightly tight, which is given as: $\log(\sigma_{*,BCG}) = (0.14 \pm 0.02)\ \log M_{200} + (2.02 \pm 0.06)$ and $\log(M_{K,BCG}) = (-0.55 \pm 0.06)\ \log M_{200} - (16.04 \pm 0.78)$ respectively. The source code is in my GitHub repository (https://github.com/jjooki/BCG-Cluster/tree/main).

Keyword: SDSS, BCG, Galaxy cluster, Dark matter halo mass, mass, velocity dispersion, magnitude
Student Number: 2014-19402

1. *Introduction*

The brightest cluster galaxy (BCG) is defined as a luminous galaxy in the central regions of galaxy clusters. Many studies used BCGs as a clue for the systematic identification of their clusters in photometric data (e.g. Abell 1958; Abell et al. 1989; Koester et al. 2007; Hao et al. 2010) The relationship between BCGs and the mass of their host clusters is an important topic in the study of galaxy formation and evolution. BCGs are the most massive and luminous galaxies in galaxy clusters and are typically located at the center of the cluster.

Some studies have shown that there is a strong correlation between the mass of a BCG and the mass of its galaxy cluster (Bellstedt et al. 2016). In general, more massive BCGs are found in more massive galaxy clusters. This relationship is thought to arise from the hierarchical structure formation process from a galaxy cluster, where smaller galaxy groups and clusters merge to form larger ones. As a result, the most massive galaxies in a galaxy cluster tend to be located at the center of the cluster, where they can accrete additional mass from surrounding galaxies.

The relationship between BCG mass and cluster mass has important implications for the study of galaxy evolution. For example, it has been shown that BCGs in more massive galaxy clusters tend to have older stellar populations and more evolved morphologies compared to BCGs in less massive clusters. This suggests that the mass of a galaxy cluster can influence the evolution of its constituent galaxies.

In addition, the relationship between BCG and cluster can provide valuable constraints on cosmological models. By comparing the observed relationship to theoretical predictions, it is possible to test the accuracy of these models and gain insights into the processes involved in galaxy formation and evolution.

Overall, the relationship between the mass of a BCG and the mass of its galaxy cluster is an important area of study in the field of astrophysics. By studying this relationship, it is possible to gain valuable insights into the formation and evolution of galaxies in different environments.

This paper suggests several galaxy cluster halo mass estimation methods by BCG properties from the photometric and spectroscopic dataset of the Sloan Digital Sky Survey-Data Release 13, so-called SDSS-dr13 (Albareti et al. 2017). I find some relations and compare them with several previous papers. Throughout the paper, I assume the standard ΛCDM model with $\Omega_m = 0.3$, $\Omega_\Lambda = 0.7$, Ω_r, $\Omega_k = 0$, $H_0 = 100\,h$ km s^{-1} Mpc^{-1} and $h_0 = 0.7$.

2. *Data Preparation*

2-1. *Cluster Sample*

Table 1
Cluster data description

Column	Description	Unit
Ng	Number of total galaxy members for this cluster	-
ClID	Cluster Identifier	-
RAJ2000	Cluster center right ascension(J2000)	deg
DEJ2000	Cluster center right ascension(J2000)	deg
z	Redshift corresponds to a no-QSO redshift	-
RV	Cluster radial velocity	km/s
CoDist	Comoving distance	$h^{-1}Mpc$
r200	Radius from the cluster center at which ρ=$\Delta 200\rho c$	$h^{-1}Mpc$
N200	Number of all member galaxies within r200	-
sig200	Velocity dispersion within r200	km/s
M200	Cluster mass within r200	$M_\odot$
Rs	NFW scale radius	$h^{-1}Mpc$
Ms	NFW scale mass	$M_\odot$
conc	Concentration = $R200/Rs$	-

Before beginning to study, a catalog with all the data of galaxy clusters and cluster members was needed for analyzing the relationship among cluster and its membership galaxies. GalWeight cluster catalog, GalWCat19 (Abdullah et al. 2019), which has 1,800 clusters and 34,471 cluster membership galaxies from z=0.001 to 0.2, is a good enough resource for studying nearby galaxy clusters.

The clusters identified from overdensities in redshift-phase space by the GalWeight technique (Abdullah et al. 2018) range in redshift between 0.01 – 0.2 and mass between $(0.4 – 14)\times 10^{14}\,h^{-1}M_\odot$ The catalog includes a large number of cluster parameters, such as sky

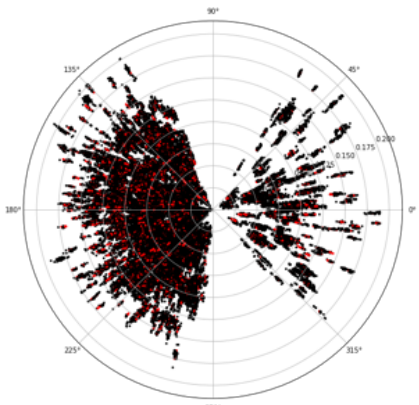

Figure 1. Light cone diagram. The black points represent the distribution of all galaxies in the SDSS sample, while the red points represent the 34,471 cluster members in the 1,800 GalWCat19 catalog clusters.

position, redshift, membership, velocity dispersion, and mass at overdensities Δ = 500, 200, 100, and 5.5 from Abdullah et al. (2018).

2-2. *Galaxy Sample*

In the GalWCat19 catalog, the data of 34, 471 member galaxies are identified within the radius at $\Delta = 200$. However, it is essential to collect more galaxy properties except for redshift because there are only redshift and coordinates in the GalWeight19 cluster membership dataset. Luminosity (or absolute magnitude) and mass of galaxies are needed for distinguishing the BCGs from the others in the cluster and investigating the BCG mass and their cluster halo mass relationship. It is uncertain which features are used for the study and have missing values, which would make the analysis harder. Thus, as many features as possible are collected, and left only a few necessary features.

Table 2
Cluster membership data description

Column	Description	Unit
ra	Right Ascension (GalWCat19)	deg
dec	Declination (GalWCat19)	deg
z	Redshift (GalWCat19)	-
mag_u	Petrosian u-band magnitude corrected for extinction	mag
mag_g	Petrosian g-band magnitude corrected for extinction	mag
mag_r	Petrosian r-band magnitude corrected for extinction	mag
mag_i	Petrosian i-band magnitude corrected for extinction	mag
mag_z	Petrosian z-band magnitude corrected for extinction	mag
velDisp	Velocity dispersion	km/s
passive_logmass	Best-fit stellar log mass of a galaxy	$M\odot$
pca_logmass	Stellar log mass measured by PCA	$M\odot$
absMagK	Absolute magnitude in K inferred from model	mag
pca_vdisp	PCA velocity dispersion	km/s
frac_ellip	debiased fraction of votes for elliptical	-
ClID	Cluster Identifier	-

Petrosian magnitudes (petroMag) in PhotoObj view are selected as a galaxy photometric magnitude. According to the SDSS official website①, petroMag is highly recommended for the photometry of nearby galaxies. Measuring the flux of galaxies is more difficult than those of stars because galaxies all have different radial surface brightness profiles. It is necessary to measure a constant fraction of the total light, independent of the position and distance of the object in order to avoid biases. To satisfy these requirements, a modified form of the Petrosian system (Petrosian 1976), measuring galaxy flux within a circular aperture whose radius is defined by the shape of the azimuthally averaged light profile, is offered by the SDSS database. In addition, the SDSS offers extinction of observed direction for each ugriz filter. Therefore, the magnitude obtained by subtracting extinction from petroMag is finally used in the study.

Redshift and velocity dispersion is loaded from the SpecObj view in the SDSS database. In some cases, a zero value of velocity dispersion came out, so PCA velocity dispersion from the stellarMassPCAWiscM11 table was also brought in as an alternative feature.

In the SDSS stellarMassPassivePort table②, there is log mass, which is the best-fit galaxy stellar mass using the method suggested by Maraston (Maraston et al. 2009). This feature could make the study easier, but this feature has many missing values. Therefore, how to fill the missing value of galaxy stellar mass is crucial to analyze the targeted relationship.

Finally, all data of features in the SDSS is loaded from the SDSS-dr13 skyserver database by a python SQL crawler with Selenium library.

3. *Data Preprocessing*

SDSS datasets have some missing values like the relationship among the galaxy properties is needed to fill the missing values in the SDSS dataset.

3-1. *Missing BCG's Data Estimation*

galactic features, like absolute K corrected magnitude, stellar velocity dispersion, and stellar mass, have some missing data on 9,091 galaxies. Fortunately, the features which have fully filled data are the photometric ones, such as the Petrosian magnitude of ugriz filters. So, a process of inferring some empty data would be thought to raise the reliability of the analysis. Since the type of BCG is elliptical, all kind of estimations in this part is about the elliptical galaxy as the fraction of elliptical is over 0.5.

3-1-1. *Absolute K-band Magnitude(M_K)*

There are all apparent magnitudes for each filter, which could be converted to absolute magnitudes. But the absolute K-band magnitude of the galaxy (M_K) offered by the SDSS-dr13 is more precious for measuring the galaxy luminosity. So, I try to infer M_K by the other magnitudes.

① https://www.sdss.org/dr13/algorithms/magnitudes/
② http://skyserver.sdss.org/dr16/en/help/browser/browser.aspx?cmd=description+Galaxy+V#&&history=description+stellarMassPassivePort+U

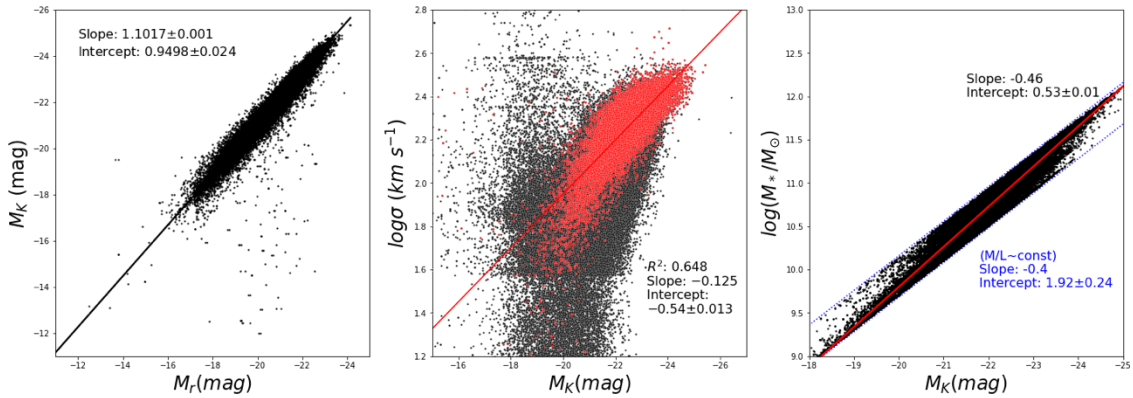

Figure 2. Plots representing the relation among elliptical galaxy properties in order to fill missing values in the SDSS data. (Left) The distribution of corrected absolute magnitude (M_K) offered by the SDSS stellarMassPassivePort table and absolute r-band magnitude (M_r) calculated by Hubble's law. (Middle) The distribution of M_K and stellar velocity dispersion (σ_*). The gray points are of all samples, while the red points are of elliptical galaxies identified by fraction of elliptical by GalaxyZoo database. (Right) The distribution of M_K and logarithm stellar mass ($\log(M_*/M_\odot)$). The red line is the best-fit result by ordinary least square (OLS) approach. The blue dashed line is best-fit result when assumed the M_*/L_* ratio is constant so that the slope is fiexd at -0.4.

First of all, apparent magnitudes are changed to the absolute magnitude with their redshift values. In order to calculate this, the relativistic Doppler effect, Friedmann Equation, Hubble's law to measure comoving distance (d in the unit of Mpc), and Pogson's equation are used. And those are respectively given by:

$$v_r(z) = \frac{(1+z)^2 - 1}{(1+z)^2 + 1} c \ (c = light\ speed) \quad (1)$$

$$h(z) = h_0\sqrt{\Omega_m(1+z)^3 + \Omega_\Lambda} \quad (2)$$

$$d = v_r(z)/100h(z) \quad (3)$$

$$M_i = m_i - 5\log(v_r/h) - 15 \ (i = u, g, i, r, z) \quad (4)$$

Utilizing all those equations, all absolute magnitudes could be calculated. The best-fit result (Fig1-1.) of executing the linear regression method through the absolute r-band magnitudes obtained in this way is as follows.

$$M_K = 1.104\, M_r + 1.023 \quad (5)$$

This regression is quite creditable since its R^2-score is 0.911. So, I adopt the relation to filling the missing absolute K-band magnitudes.

3-1-2. *Velocity Dispersion*

In the case of an elliptical galaxy, stellar velocity dispersion(σ_*) is a significant property to explain elliptical galaxy stellar mass by the virial theorem. Therefore, σ_* should be contained in final feature lists for galaxy cluster halo mass prediction. But a pretty amount of measured σ_* in the SDSS-dr13 database have wrong specific values like 0 or 850($km\ s^{-1}$) for unknown reason.

According to the research of Faber and Jackson (Faber et al. 1976), luminosity follows a power law of stellar dispersion velocity, $L_* \sim \sigma^4$. Then this relation could be changed by the Pogson equation as given by:

$$log\sigma_* = -0.1M_K + \alpha \quad (6)$$

Since de Vaucouleurs law is the special case of the Sersic profile, this relation is not always explained about the elliptical galaxy. Though, velocity dispersion and luminosity, which could alter the absolute magnitude, still follow the power law close to a case of n=4.

$$log\sigma_* = -0.125\, M_K - 0.540 \quad (7)$$

This is the best-fit linear relation derived by given data. It is as same as $L_* \sim \sigma^{3.21}$

3-1-3. *Stellar Mass*

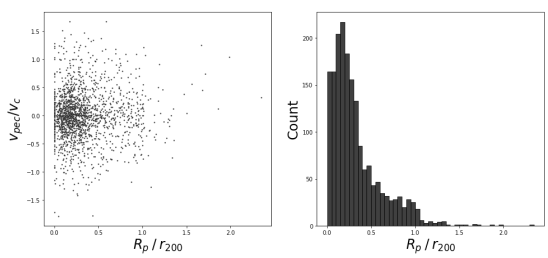

Figure 3. (Left) The normalized diagram of BCGs for each cluster field. (Right) The position distribution of BCGs.

I could obtain the logarithm mass ($\log(M_*/M_\odot)$) of almost galaxies from the SDSS but some data is empty so that should fill in the blank. The well-known M-L relation among stellar mass(M_*) and stellar luminosity(L_*) of elliptical galaxies, is required to estimate the rest of log mass ($M_*/L_* = const$; de

Vaucouleurs. 1953). M_K related to its luminosity is given by (Pogson, N. 1856):

$$M_K - M_{K,\odot} = -2.5 log L_*/L_\odot \quad (8)$$

According to a previous paper (Willmer. 2018), the absolute K-band solar magnitude is 3.27 ($M_{K,\odot} = 3.27$), so (6) equation converts to $M_K = -2.5 log L_* + 3.27$, where L_* in a unit of $L_\odot$. Then, expressing the M-L relation ($M_*/L_* = \alpha$)differently, it is given as:

$$log M_* = -0.4 M_K + 1.31 + log\alpha \quad (9)$$

When assuming the M_*/L_* ratio is constant, the slope of a power law is fixed at -0.4. In this case, the best-fit result for these variables from the ordinary least square (OLS) approach is $log\alpha = 0.61 \pm 0.24$. So, the mass-luminosity ratio is

$$M_*/L_* \sim 4^{+3.1}_{-1.7} \quad (10)$$

On the other hand, the best-fit result without the assumption about M_*/L_* relation is

$$log M_* = -0.46 M_K + (0.53 \pm 0.01) \quad (11)$$

3-2. *Identification & Properties of the BCGs*

Before the analysis of BCGs, it should be processed to classify the BCG. Typically, BCGs are chosen by photometric technique (Lauer et al. 2014). Nowadays, a galaxy with the highest stellar mass in the cluster has been selected instead of a galaxy with the smallest magnitude in a specific photometric band (Gozaliasl et al. 2019). However, the original approach is used to identify BCGs from the cluster members since magnitude is observed data, while mass is estimated data. It is thought that it must be a directly obtained value, in order to be a characteristic representing something.

Here, the BCG is defined with the absMagK feature, which is strongly related to r-band absolute magnitude. Positional constraint to select the BCG, which is located within 0.5 R_{200} (Sohn et al. 2019) is not adopted since the position distribution of galaxy clusters is also worth researching in the future.

Without any constraint, it is examined the properties of the BCGs including stellar mass, stellar velocity dispersion, peculiar velocity, and relative position in their host clusters. First, the mean and median values of R_p (projected radius)-to-r_{200} (radius from the cluster center at which ρ=$\Delta 200 \rho c$) from the center is 0.23, 0.32 respectively, while those of cluster membership galaxies are 3.58, 3.74. This means that BCGs are located nearby the center of their hosts. In addition, their relativistic peculiar velocity average is lower than other galaxies. Fig3 and Fig4 show the features mentioned above well.

4. *Cluster mass and BCG relations*

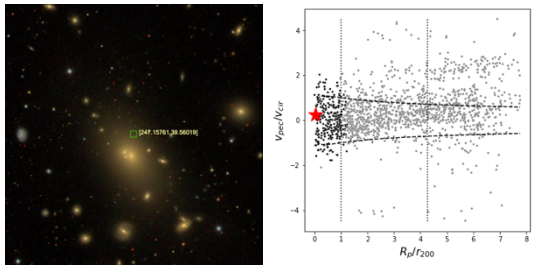

Figure 4. (Right) Sample galaxy cluster image in the SDSS object explorer. (Left) R-v plot representing the BCG's properities - low peculiar velocity and position nearby the galaxy cluster center.

GalWCat19 catalog clusters have information for examining relations between BCG and the mass of their host clusters. Other BCG properties, such as stellar mass, stellar dispersion, and absolute magnitude, are used to approximate cluster mass. Here we explore the relations among these properties. The OLS approach is chosen for all kinds of linear regression in this paper.

4-1. $M_{*,BCG} - M_{200}$ *Relations*

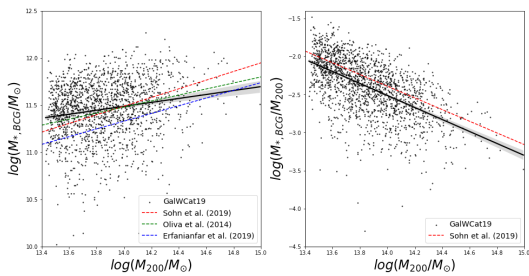

Figure 5. (a) Plot stellar masses of BCGs as a function of M_{200}. The black solid line is the best-fit relation I derive for the GalWCat19 clusters. Another three dashed lines are the $M_{*,BCG} - M_{200}$ relation from previous works, which are successively Sohn et al. (2019) (red line), Oliva-Altamirano et al. (2014) (green line) and Erfanianfar et al. (2019) (blue line). (b) The ratio between $M_{*,BCG}$ and M_{200} as a function of M_{200}. The black solid line the best-fit result from GalWCat19 clusters. The red line is the relation from Sohn et al. (2019).

Figure 5 (a) shows the mass-mass relations. The best-fit relation (black solid line in Figure 6 (a)) between the BCG stellar mass and the cluster dynamical mass is:

$$log(M_{*,BCG}/M_\odot) = (0.21 \pm 0.03) log(M_{200}/M_\odot) + (8.55 \pm 0.37) \quad (12)$$

Previous observations show similar relations based on several cluster samples in the similar mass and redshift range of $M_{200} > 0.4 \times 10^{14} M_\odot$, $z < 0.3$ respectively. There are some differences in the regression result due to the usage of different cluster samples. The slope of the relation from another research is in Table 3:

Table 3

The slopes of $M_{*,BCG} - M_{200}$ relation

Paper	Slope
Park. (2022)	0.21±0.03
Sohn et al. (2019)	0.46±0.03
Oliva-Altamirano et al. (2014)	0.32±0.09
Erfanianfar et al. (2019)	0.41±0.04

Another important relationship is the ratio between $M_{*,BCG}$ and M_{200} as a function of cluster halo mass (Sohn et al. 2019). Although there are some best-fit relations, they have a common fact: a low Spearman correlation coefficient. So, a statistical technique is needed to raise the explanatory power. Sohn et al. (2019) suggests the method by analyzing the ratio between BCG stellar mass and the cluster halo mass as a function of halo mass.

Figure 5 (b) shows this transformed result. The red line is a comparison relation by Sohn et al. (2019), which raises the absolute Spearman correlation coefficient from 0.32 to 0.68. The best-fit relation for the GalWCat19 clusters is given as:

$$log(M_{*,BCG}/M_{200}) = (-0.79 \pm 0.03) log(M_{200}/M_{\odot}) + (8.55 \pm 0.37) \quad (13)$$

The slope of the relationship is consistent with the relation in the literature: e.g. the coefficient is -0.77±0.12 and the intercept is 8.39±4.05 from Sohn et al. (2019)

4-2. $\sigma_{*,BCG} - M_{200}$ Relations

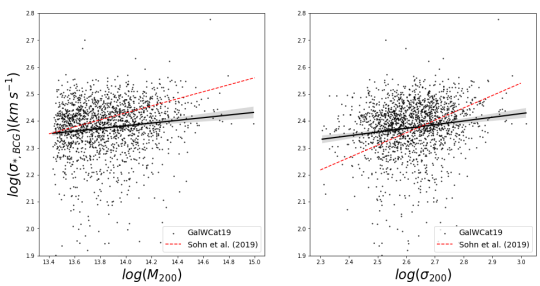

Figure 6. (a) Plot about stellar velocity dispersion of BCGs as a function of M_{200}. (b) Plot about $\sigma_{*,BCG}$ as a function of σ_{200}. Both black solid line are the best-fit result from GalWCat19 clusters for each plot. Both red dashed line are the relation from Sohn et al. (2019).

It could be thought that the relation between $\sigma_{*,BCG}$ and M_{200} is also established as that of $M_{*,BCG}$ and M_{200} since the stellar mass is calculated with central velocity dispersion by the virial theorem. Interestingly, certain studies said that the stellar velocity dispersion of the central galaxy is related to its halo mass (Zahid et al. 2016, 2018). Figure 6 (a) is the regression result of the relation suggested by Zahid et al. (2016). The result is told $\sigma_{*,BCG}$ correlates well with M_{200}. The best-fit relation for the GalWCat19 clusters is:

$$log\sigma_{*,BCG} = (0.14 \pm 0.02) log(M_{200}/M_{\odot}) + (2.02 \pm 0.06) \quad (14)$$

Through two equations (11) and (13), It can be seen that there is a power law of $M_* - \sigma_*$ similar as the virial theorem ($M_* \sim \sigma_*^2$). Compared to other studies by Sohn et al. (2019), the slope of the relation is slightly different. This point will have to be studied further in the future.

4-3. $L_{*,BCG} - M_{200}$ Relations

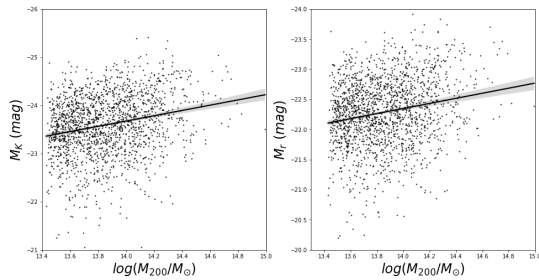

Figure 7. (a) Plot absolute K magnitude (M_K) of BCGs given by the SDSS and cluster halo mass (M_{200}). (b) Plot about absolute r-band Petrosian magnitude as a function of M_{200}.

The easiest way to predict the cluster halo mass is estimation with the photometric magnitude of its BCGs. Even though spectroscopic data is offered by many previous surveys, photometric data is much better than spectroscopic data for mass estimation using computer vision (CV), where researchers could get results from a single picture. Therefore, the relation between BCG magnitude and cluster mass is worthwhile with the photometric redshift estimation method (Benitez. 2000; Brammer et al. 2008; Sadeh et al. 2016).

Figure 7 (a) and (b) show the distribution of BCG luminosity and cluster mass. With absolute K and r band magnitudes, the best-fit relation for the GalWCat19 is given as:

$$M_{K,BCG} = (-0.55 \pm 0.06) log(M_{200}/M_{\odot}) - (16.0 \pm 0.78) \quad (15)$$

$$M_{r,BCG} = (-0.42 \pm 0.05)\, log(M_{200}/M_{\odot}) - (16.5 \pm 0.70) \quad (16)$$

This means that there is a correlation between BCG luminosity and cluster dynamical mass. It can be seen impressive results.

5. *Discussion*

First, one of the typical methods to measure the mass of a galaxy cluster (M_{cl}) is the virial theorem. This is based on the fact that the virial mass of a gravitationally bound system is related to the velocity dispersion of its constituent particles through the equation: $M_{cl,vir} = (3\pi/G)\sigma_v^2 R_{vir}$. However, the virial mass measurement from scratch is a complicated process. For instance, to obtain the velocity dispersion of galaxies within a galaxy cluster, a process of classifying if they are members of the galaxy cluster is first necessary. Through this process, it is thought that cluster membership identification and

velocity dispersion calculation are not easy because various physical techniques should be used.

Therefore, the primary aim of this paper is to suggest a way to estimate nearby galaxy cluster ($z < 0.2$) halo mass with only BCG photometric and spectroscopic properties, such as Petrosian magnitude, redshift, and velocity dispersion, from the SDSS dataset. It is sufficient to accomplish the targeted goal with all relations proposed in this paper. Of course, there is some regret in the analysis since several techniques, like Bayesian, MCMC and so on, to increase accuracy were not used.

In the future, this work is used for cluster mass prediction with Deep Learning from only the original photometric images. It is believed that a well-trained open-source deep learning model would make the investigators study the field of galaxy and galaxy cluster easily.

6. *Reference*

[1] Abdullah, M. H., Wilson, G., & Klypin, A. (2018). GalWeight: A New and Effective Weighting Technique for Determining Galaxy Cluster and Group Membership. The Astrophysical Journal, 861(1), 22.

[2] Abdullah, M. H., Wilson, G., Klypin, A., Old, L., Praton, E., & Ali, G. B. (2020). GalWeight Application: A Publicly Available Catalog of Dynamical Parameters of 1800 Galaxy Clusters from SDSS-DR13, (GalWCat19). The Astrophysical Journal Supplement Series, 246, 2. https://doi.org/10.3847/1538-4365/ab536e

[3] Albareti, F. D., Prieto, C. A., Almeida, A., Anders, F., Anderson, S., Andrews, B. H., Aragón-Salamanca, A., Argudo-Fernández, M., Armengaud, E., & Aubourg, E. (2017). The 13th data release of the Sloan Digital Sky Survey: First spectroscopic data from the SDSS-IV survey mapping nearby galaxies at Apache Point Observatory. The Astrophysical Journal Supplement Series, 233(2), 25.

[4] Bellstedt, S., Lidman, C., Muzzin, A., Franx, M., Guatelli, S., Hill, A., Hoekstra, H., Kurinsky, N., Labbe, I., Marchesini, D., Marsan, Z. C., Safavi-Naeini, M., Sifon, C., Stefanon, M., Sande, J., Dokkum, P., & Weigel, C. (2016). The evolution in the stellar mass of Brightest Cluster Galaxies over the past 10 billion years. Monthly Notices of the Royal Astronomical Society, 460. https://doi.org/10.1093/mnras/stw1184

[5] Benitez, N. (2000). Bayesian photometric redshift estimation. The Astrophysical Journal, 536(2), 571.

[6] Brammer, G. B., van Dokkum, P. G., & Coppi, P. (2008). EAZY: a fast, public photometric redshift code. The Astrophysical Journal, 686(2), 1503.

[7] Dalal, R., Strauss, M. A., Sunayama, T., Oguri, M., Lin, Y.-T., Huang, S., Park, Y., & Takada, M. (2021). Brightest cluster galaxies are statistically special from $z = 0.3$ to $z = 1$. Monthly Notices of the Royal Astronomical Society, 507(3), 4016-4029. https://doi.org/10.1093/mnras/stab2363

[8] de Vaucouleurs, G. (1953). On the Distribution of Mass and Luminosity in Elliptical Galaxies. Monthly Notices of the Royal Astronomical Society, 113(2), 134-161. https://doi.org/10.1093/mnras/113.2.134

[9] Erfanianfar, G., Finoguenov, A., Furnell, K., Popesso, P., Biviano, A., Wuyts, S., Collins, C. A., Mirkazemi, M., Comparat, J., Khosroshahi, H., Nandra, K., Capasso, R., Rykoff, E., Wilman, D., Merloni, A., Clerc, N., Salvato, M., Chitham, J. I., Kelvin, L. S., . . . Kukkola, A. (2019). Stellar mass-halo mass relation for the brightest central galaxies of X-ray clusters since $z \sim 0.65$. Astronomy and Astrophysics, 631, A175. https://doi.org/10.1051/0004-6361/201935375

[10] Faber, S. M., & Jackson, R. E. (1976). Velocity dispersions and mass-to-light ratios for elliptical galaxies. The Astrophysical Journal, 204, 668-683. https://doi.org/10.1086/154215

[11] Gozaliasl, G., Finoguenov, A., Tanaka, M., Dolag, K., Montanari, F., Kirkpatrick, C. C., Vardoulaki, E., Khosroshahi, H. G., Salvato, M., & Laigle, C. (2019). Chandra centres for COSMOS X-ray galaxy groups: differences in stellar properties between central dominant and offset brightest group galaxies. Monthly Notices of the Royal Astronomical Society, 483(3), 3545-3565.

[12] Lauer, T. R., Postman, M., Strauss, M. A., Graves, G. J., & Chisari, N. E. (2014). Brightest Cluster Galaxies at the Present Epoch. The Astrophysical Journal, 797, 82. https://doi.org/10.1088/0004-637x/797/2/82

[13] Oliva-Altamirano, P., Brough, S., Lidman, C., Couch, W. J., Hopkins, A. M., Colless, M., Taylor, E., Robotham, A. S. G., Gunawardhana, M. L. P., Ponman, T., Baldry, I., Bauer, A. E., Bland-Hawthorn, J., Cluver, M., Cameron, E., Conselice, C. J., Driver, S., Edge, A. C., Graham, A. W., . . . Sharp, R. G. (2014). Galaxy And Mass Assembly (GAMA): testing galaxy formation models through the most massive galaxies in the Universe. Monthly Notices of the Royal Astronomical Society, 440(1), 762-775. https://doi.org/10.1093/mnras/stu277

[14] Petrosian, V. (1976). Surface Brightness and Evolution of Galaxies. The Astrophysical Journal, 210, L53. https://doi.org/10.1086/182301

[15] Pogson, N. (1856). Magnitudes of Thirty-six of the Minor Planets for the First Day of each Month of the Year 1857. Monthly Notices of the Royal Astronomical Society, 17(1), 12-15. https://doi.org/10.1093/mnras/17.1.12

[16] Sadeh, I., Abdalla, F. B., & Lahav, O. (2016). ANNz2: photometric redshift and probability distribution function estimation using machine learning. Publications of the Astronomical Society of the Pacific, 128(968), 104502.

[17] Sohn, J., Geller, M. J., Diaferio, A., & Rines, K. J. (2020). Velocity Dispersions of Brightest Cluster Galaxies and Their Host Clusters. The Astrophysical Journal, 891(2), 129.

[18] Sohn, J., Geller, M. J., Zahid, H. J., Fabricant, D. G., Diaferio, A., & Rines, K. J. (2017). The velocity dispersion function of very massive galaxy clusters: Abell 2029 and Coma. The Astrophysical Journal Supplement Series, 229(2), 20.

[19] Survey, S. D. S. Measures of Flux and Magnitude. https://www.sdss.org/dr13/algorithms/magnitudes/

[20] Willmer, C. N. A. (2018). The Absolute Magnitude of the Sun in Several Filters. The Astrophysical Journal Supplement Series, 236(2), 47. https://doi.org/10.3847/1538-4365/aabfdf

[21] Zahid, H. J., Geller, M. J., Fabricant, D. G., & Hwang, H. S. (2016). The scaling of stellar mass and central stellar velocity dispersion for quiescent galaxies at z< 0.7. The Astrophysical Journal, 832(2), 203.

[22] Zahid, H. J., Sohn, J., & Geller, M. J. (2018). Stellar velocity dispersion: Linking quiescent galaxies to their dark matter halos. The Astrophysical Journal, 859(2), 96.